

University of Nebraska - Lincoln

DigitalCommons@University of Nebraska - Lincoln

---

Faculty Publications in Food Science and  
Technology

Food Science and Technology Department

---

2020

## Identification of Simplified Microbial Communities That Inhibit *Clostridioides difficile* Infection through Dilution/Extinction

Jennifer M. Auchtung

Eva C. Preisner

James Collins

Armando I. Lerma

Robert A. Britton

Follow this and additional works at: <https://digitalcommons.unl.edu/foodsciefacpub>



Part of the [Food Science Commons](#)

---

This Article is brought to you for free and open access by the Food Science and Technology Department at DigitalCommons@University of Nebraska - Lincoln. It has been accepted for inclusion in Faculty Publications in Food Science and Technology by an authorized administrator of DigitalCommons@University of Nebraska - Lincoln.



# Identification of Simplified Microbial Communities That Inhibit *Clostridioides difficile* Infection through Dilution/Extinction

 Jennifer M. Auchtung,<sup>a,b,c,d</sup> Eva C. Preisner,<sup>a,b</sup> James Collins,<sup>a,b\*</sup> Armando I. Lerma,<sup>a,b\*</sup>  Robert A. Britton<sup>a,b</sup>

<sup>a</sup>Alkek Center for Metagenomics and Microbiome Research, Baylor College of Medicine, Houston, Texas, USA

<sup>b</sup>Department of Molecular Virology and Microbiology, Baylor College of Medicine, Houston, Texas, USA

<sup>c</sup>Nebraska Foods for Health Center, University of Nebraska—Lincoln, Lincoln, Nebraska, USA

<sup>d</sup>Department of Food Science and Technology, University of Nebraska—Lincoln, Lincoln, Nebraska, USA

**ABSTRACT** The gastrointestinal microbiome plays an important role in limiting susceptibility to infection with *Clostridioides difficile*. To better understand the ecology of bacteria important for *C. difficile* colonization resistance, we developed an experimental platform to simplify complex communities of fecal bacteria through dilution and rapidly screen for their ability to resist *C. difficile* colonization after challenge, as measured by >100-fold reduction in levels of *C. difficile* in challenged communities. We screened 76 simplified communities diluted from cultures of six fecal donors and identified 24 simplified communities that inhibited *C. difficile* colonization *in vitro*. Sequencing revealed that simplified communities were composed of 19 to 67 operational taxonomic units (OTUs) and could be partitioned into four distinct community types. One simplified community could be further simplified from 56 to 28 OTUs through dilution and retain the ability to inhibit *C. difficile*. We tested the efficacy of seven simplified communities in a humanized microbiota mouse model. We found that four communities were able to significantly reduce the severity of the initial *C. difficile* infection and limit susceptibility to disease relapse. Analysis of fecal microbiomes from treated mice demonstrated that simplified communities accelerated recovery of indigenous bacteria and led to stable engraftment of 19 to 22 OTUs from simplified communities. Overall, the insights gained through the identification and characterization of these simplified communities increase our understanding of the microbial dynamics of *C. difficile* infection and recovery.

**IMPORTANCE** *Clostridioides difficile* is the leading cause of antibiotic-associated diarrhea and a significant health care burden. Fecal microbiota transplantation is highly effective at treating recurrent *C. difficile* disease; however, uncertainties about the undefined composition of fecal material and potential long-term unintended health consequences remain. These concerns have motivated studies to identify new communities of microbes with a simpler composition that will be effective at treating disease. This work describes a platform for rapidly identifying and screening new simplified communities for efficacy in treating *C. difficile* infection. Four new simplified communities of microbes with potential for development of new therapies to treat *C. difficile* disease are identified. While this platform was developed and validated to model infection with *C. difficile*, the underlying principles described in the paper could be easily modified to develop therapeutics to treat other gastrointestinal diseases.

**KEYWORDS** *Clostridioides difficile*, FMT, colonization resistance, microbiome, simplified communities

*Clostridioides difficile* is the most common cause of antibiotic-associated diarrhea (1–3). Estimates of annual health care costs associated with treating *C. difficile* infection (CDI) in the United States range from \$1 billion to \$4.8 billion (4). Although

**Citation** Auchtung JM, Preisner EC, Collins J, Lerma AI, Britton RA. 2020. Identification of simplified microbial communities that inhibit *Clostridioides difficile* infection through dilution/extinction. mSphere 5:e00387-20. <https://doi.org/10.1128/mSphere.00387-20>.

**Editor** Vincent B. Young, University of Michigan—Ann Arbor

**Copyright** © 2020 Auchtung et al. This is an open-access article distributed under the terms of the [Creative Commons Attribution 4.0 International license](https://creativecommons.org/licenses/by/4.0/).

Address correspondence to Robert A. Britton, [robert.britton@bcm.edu](mailto:robert.britton@bcm.edu).

\* Present address: James Collins, Department of Microbiology & Immunology, University of Louisville School of Medicine, Louisville, Kentucky, USA; Armando I. Lerma, Department of Food Science and Technology, University of Nebraska—Lincoln, Lincoln, Nebraska, USA.

For a commentary on this article, see <https://doi.org/10.1128/mSphere.00701-20>.

**Received** 27 April 2020

**Accepted** 1 July 2020

**Published** 29 July 2020

uncomplicated infections are typically self-limiting, severe infections require treatment (5). For approximately 25% of patients, resolution of primary infection is followed by one or more rounds of recurrent *C. difficile* infection (rCDI) (6), which diminishes the quality of life and contributes to overall health care costs (7, 8).

To cause disease, ingested *C. difficile* spores must germinate into vegetative cells that produce toxins. The bile salt cholate and its derivatives stimulate *C. difficile* germination, along with cogerminants glycine and other amino acids (9, 10). The gastrointestinal microbiome plays key roles in limiting symptomatic CDI by competing with *C. difficile* for nutrients (11–13), producing metabolites that inhibit *C. difficile* growth (14–18), maintaining immune homeostasis (19–21), and metabolizing primary bile salts into secondary bile salts that inhibit the growth of vegetative cells (9, 22, 23). Antibiotic treatment leads to loss of GI microbiome diversity (24–26), is a key risk factor for primary infection (27–30), and contributes to susceptibility to recurrent disease.

Several different therapies are currently used to treat rCDI and act to limit different aspects of cell growth and pathogenicity. Clinical cure rates of 70% have been reported following extended-pulsed administration of the antibiotic fidaxomicin (31). An 80% cure rate has been reported for patients with primary and recurrent CDI treated with bezlotoxumab, an antibody that targets *C. difficile* toxin B (32). Fecal microbiome transplantation (FMT) for treatment of rCDI has reported cure rates from 44 to 100% (33, 34). However, concern for potential adverse events (for examples, see reference 35) motivates ongoing studies to develop alternatives to FMT to treat rCDI.

Defined community microbial therapeutics are one alternative to FMT under investigation. Previous studies have demonstrated success in administration of a consortium of 10 (36) or 33 (37) human fecal bacteria for treatment of rCDI. Despite these advances, no defined microbial therapeutic is currently available for treatment of CDI. One limitation to developing microbial community therapeutics is the availability of appropriate models for rapid screening. We developed a coupled *in vitro* and *in vivo* platform to screen simple microbial communities for their ability to prevent CDI. We identified four simplified communities that limited *C. difficile* growth *in vitro* and reduced the severity of disease *in vivo*. While the potential of these communities to treat disease in humans is unknown, the approaches could be applied to identification of additional simplified communities to treat rCDI and microbiome-linked diseases.

## RESULTS

**Identification of simplified communities that limit *C. difficile* growth *in vitro*.** To identify simplified communities that could suppress *C. difficile*, we applied a dilution/extinction strategy (38, 39) as outlined in Fig. 1A. In this approach, undiluted fecal communities are simplified through dilution, with abundant organisms preserved and rare organisms randomly distributed or lost as predicted by the Poisson distribution.

Undiluted fecal communities were established in minibioreactor arrays (MBRAs) from six individual fecal donors (D1 to D6) and allowed to stabilize (Fig. 1A). Cell density was measured by nonselective plating and used with published operational taxonomic unit (OTU) abundance data (40) to estimate dilutions needed to simplify communities. Following dilution, simplified communities were stabilized in continuous culture before challenge with  $10^4$  vegetative *C. difficile* cells. We measured *C. difficile* proliferation in each bioreactor over time and identified nine simplified communities that lowered *C. difficile* levels  $>10,000$  times and 15 communities that decreased *C. difficile* levels  $>100$  times compared to *C. difficile* cultivated alone in bioreactors (Fig. 1B).

**CDI-resistant simplified communities separate into distinct community types.** To better understand how dilution impacted community composition, we compared the 16S rRNA gene content between a subset of undiluted donor communities (D2 to D4) and *C. difficile*-resistant simplified communities (SC1 to SC5) (Fig. 1C). The median number of OTUs in the undiluted communities was 67; dilution reduced the median numbers of OTUs to 50 and 42 in the simplified communities diluted  $10^{-4}$  and  $10^{-5}$ , respectively (Fig. 2A).

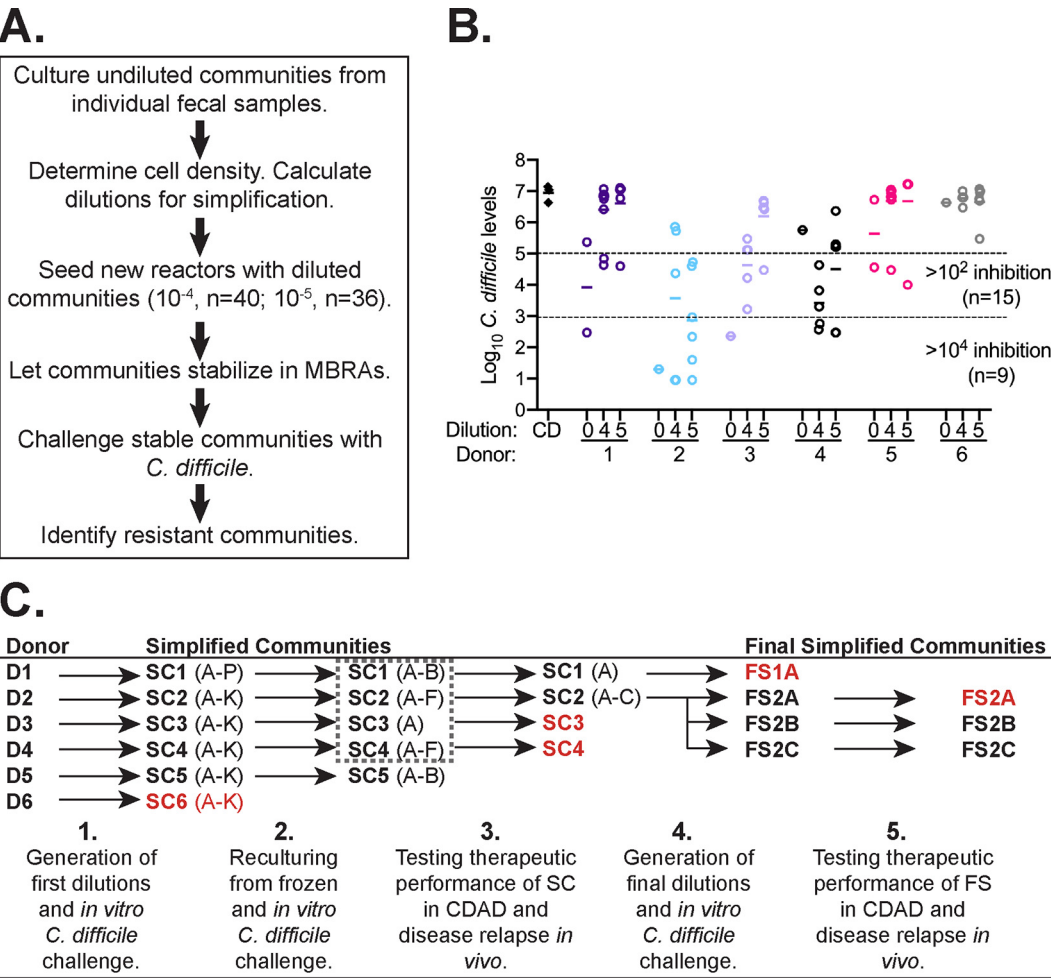


**FIG 1** Identification of simplified communities that inhibit *C. difficile* proliferation through dilution/extinction community assembly. (A) Overview of process to identify simplified communities. (B) Log<sub>10</sub> *C. difficile* levels measured in diluted communities on day 5 or 6 following challenge. Closed triangles, *C. difficile* (CD) cultured alone; open circles, *C. difficile* cultured in the presence of undiluted communities (0) and communities diluted  $10^{-4}$  (4) and  $10^{-5}$  (5) cultured from indicated fecal sample donors. Solid lines represent geometric means of samples. Dashed lines demarcate inhibition of *C. difficile* levels by  $10^2$  and  $10^4$ , with the number of samples per category indicated. (C) Schematic representation of samples generated over the course of experiments as described in the text. Red typeface indicates samples that failed to provide protection from *C. difficile* colonization at the step indicated.

We compared differences in community structure across simplified communities (Fig. 2C) and used Dirichlet multinomial mixtures to identify community types and discriminatory taxa (41) (Fig. 2D). We found that the data best partitioned into four community types, with community type A containing SC1 and SC5 communities, while SC2, SC3, and SC4 separated into community types B to D, respectively.

Forty-five OTUs accounted for 80% of the difference between community types in the model (Fig. 2D). Many of these OTUs were present in all samples, but they varied in abundance by community type. Notable features of community type A included *Bacteroides*, *Peptostreptococcaceae*, and *Lachnospiraceae* OTUs. *Peptostreptococcaceae* number 31, which was detected in 3 of 4 type A communities, was 100% identical to *C. difficile* 16S rRNA, indicating potential experimental contamination of these communities prior to *C. difficile* challenge. Type B communities had higher levels of *Anaerostipes*, *Clostridium sensu stricto*, *Clostridium* XI, and *Peptoniphilus*; *Akkermansia*, *Blautia*, *Clostridium* XVIII, and *Enterococcus* were enriched in type C communities; and *Acidaminococcus*, *Bilophila*, and *Fusobacterium* were enriched in type D communities.

**Simplified communities retain the ability to suppress *C. difficile* when recultured.** We selected 17 of the 24 *C. difficile*-resistant SC1 to SC5 cultures for retesting

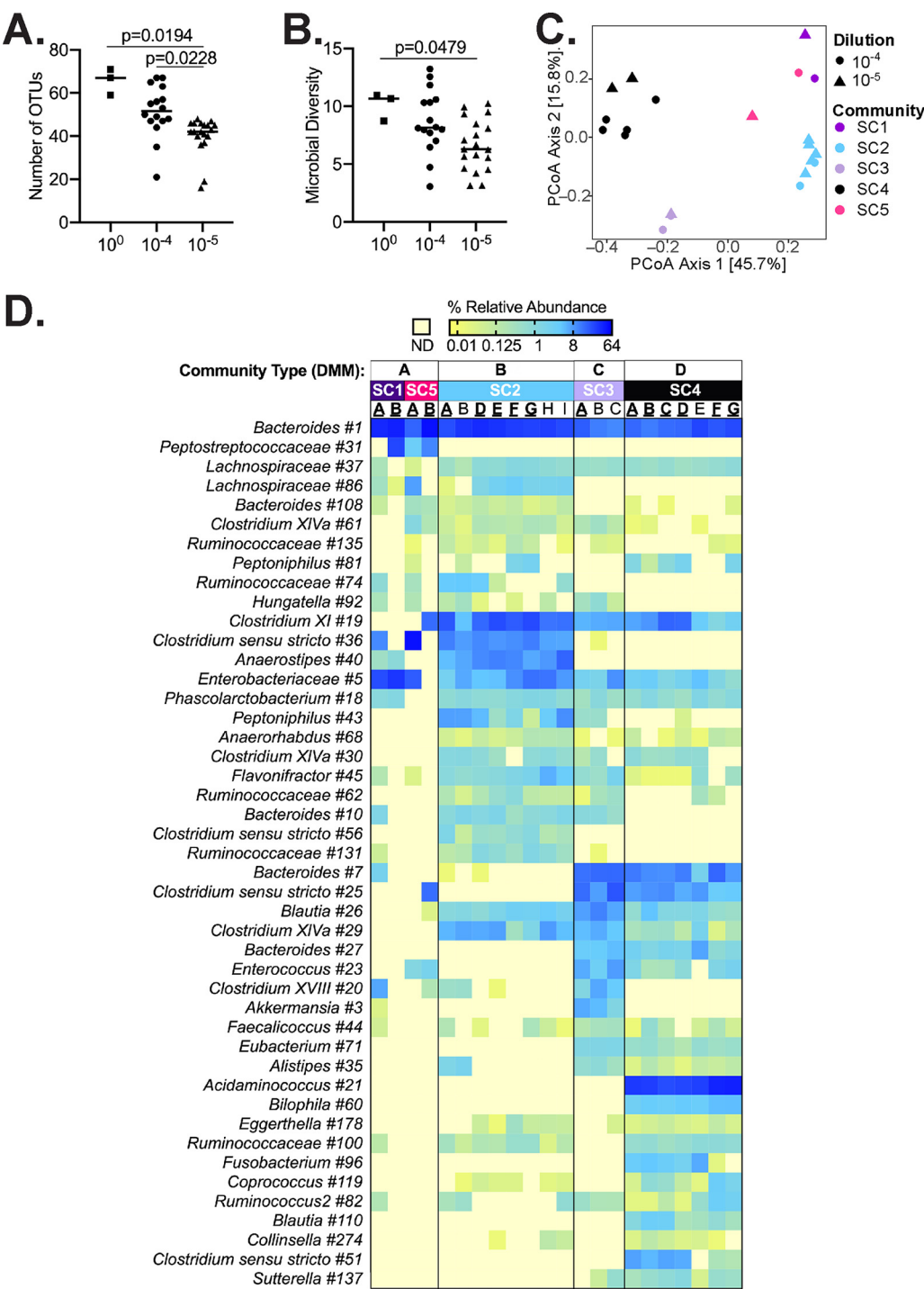


**FIG 2** Comparison of microbial communities present in undiluted and simplified communities that inhibit *C. difficile* growth. (A and B) The number of OTUs (A) and microbial diversity (inverse Simpson) (B) detected in undiluted communities (squares) and communities diluted  $10^{-4}$  (circles) and  $10^{-5}$  (triangles) are plotted. Lines represent medians; *P* values of  $<0.05$  as calculated by one-way Kruskal-Wallis testing are reported. (C) Principal-coordinate analysis (PCoA) visualization of Bray-Curtis dissimilarities between *C. difficile*-resistant communities SC1 to SC5. Colors represent different SCs as indicated; dilutions are indicated by shapes. Percent variation described by each axis is indicated in parentheses. (D) Forty-five OTUs that most significantly contribute to partitioning of SC1 to SC5 into the indicated four community types (A to D). The  $\log_2$ -transformed percent abundance of each OTU is plotted across all samples. Samples are arranged by donor and community type as indicated at the top. Values ranged from 0.01% (yellow) to 64% (dark blue) of total sequences as indicated; pale yellow indicates that there were no detected sequences (ND). Simplified community replicate names are indicated in boldface, underlining indicates communities selected for reculturing as described in the text. Table S1 contains data from all 147 OTUs that account for differences between community types.

based on previous ability to suppress *C. difficile* growth (9/9 that suppressed  $>10^4$ ; 8/24 that suppressed  $>10^2$ ) and variation in microbiome composition (indicated by boldface type in Fig. 2D). Simplified communities were established from frozen stocks in triplicate MBRAs and allowed stabilization prior to challenge with *C. difficile*. Thirteen of the 17 communities were able to inhibit *C. difficile* upon reculturing (Fig. 1C; see also Fig. S1 in the supplemental material). Five communities suppressed *C. difficile* growth  $>10,000$ -fold across all three replicates, two suppressed *C. difficile*  $>100$ -fold across all three replicates, and six communities suppressed *C. difficile* in at least one replicate (Fig. S1). We selected one replicate from each community type described in Fig. 2D that was also able to suppress *C. difficile* upon reculturing to test in a mouse model of disease. SC1A, SC2A, SC3A, and SC4A replicates were selected; replicate names were simplified to SC1 to SC4 for testing in mice.

**SC1 and SC2 suppress CDAD.** We tested SC1 to SC4 for the ability to suppress *C. difficile*-associated disease (CDAD) in a humanized microbiota mouse (<sup>HMB</sup>mouse) model of disease (42). Two positive controls were used to test for suppression of CDAD: FMT freshly prepared from our colony of <sup>HMB</sup>mice (M-FMT) and a cryopreserved aliquot of human FMT previously used successfully in a CDI fecal transplant program (H-FMT; T. Savidge, personal communication). Mice were treated with antibiotics to disrupt the microbiome and then gavaged with cells from simplified communities SC1 to SC4, M-FMT, or H-FMT on 3 consecutive days; control mice were treated with a vehicle (phosphate-buffered saline [PBS]) (Fig. 3A). Body mass was measured daily beginning with the first day of gavage to test for potential toxicity of communities. Because mice treated with SC4 exhibited  $\sim 5\%$  body mass loss from baseline prior to *C. difficile* challenge (Fig. 3B), they were excluded from further analyses.

Following *C. difficile* challenge, mice treated with PBS exhibited a decline in body mass (Fig. 3C) and shed *C. difficile* in their feces (Fig. 3E). In contrast, SC1-treated mice maintained their body mass, with levels similar to those observed in the two positive controls, M-FMT- and H-FMT-treated mice (Fig. 3C), and exhibited more rapid clearance of *C. difficile* in feces (Fig. 3E). Trends toward reduced body mass loss in SC2- and SC3-treated mice (Fig. 3C) and more rapid clearance of *C. difficile* in feces of SC2-treated mice (Fig. 3E) were not statistically significant.

Because *C. difficile* was cleared more rapidly in SC1- and SC2-treated mice, we tested whether these communities would reduce susceptibility to recurrent disease. Previously, we demonstrated that relapse could be induced through a single intraperitoneal (i.p.) injection of clindamycin (42). Four weeks following the initial *C. difficile* challenge, the majority of mice no longer shed *C. difficile* at detectable levels in their feces (Fig. 3E). We treated mice with a single clindamycin i.p. injection and then measured changes in body mass and *C. difficile* levels. Consistent with relapse, we observed a modest body mass decline (Fig. 3D) and an increase of *C. difficile* in feces (Fig. 3E) of PBS-treated mice. In contrast, there was a modest body mass gain, reduced shedding of *C. difficile* in feces, and more rapid clearance of *C. difficile* in SC1- and SC2-treated mice following relapse. M-FMT- and H-FMT-treated mice had a more modest body mass gain that was not statistically significant from the mass of PBS-treated mice.

**SC2 can be further simplified and still inhibit *C. difficile* growth.** To test whether either SC1 or SC2 could be further simplified, cultures were diluted to a concentration of 250 CFU/ml ( $10^{-6}$  dilution); Poisson calculations indicated that this dilution should reduce the complexities of SC1 and SC2 to 17 and 31 OTUs, respectively. Final simplified communities (FS) were allowed to stabilize prior to challenge with *C. difficile*. Although  $10^{-6}$  dilutions of SC1 (designated FS1A to -E) lost the ability to inhibit *C. difficile*,  $10^{-6}$  dilutions of SC2 (designated FS2A to -E) continued to inhibit *C. difficile* growth (Fig. 4A). *C. difficile* inhibition was lost when SC2 communities were diluted another 10-fold.

We analyzed the effects of further simplification on community composition and found that the number of OTUs declined from a median of 60 in SC2 cultures to medians of 28 and 9 in communities diluted  $10^{-6}$  and  $10^{-7}$  (Fig. 4B). In addition,



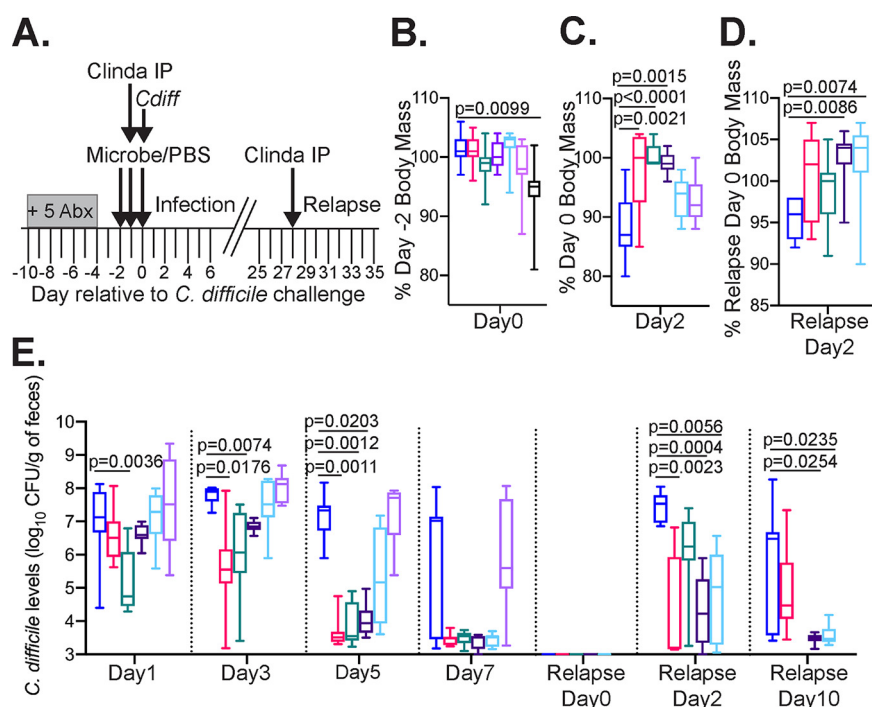


**FIG 3** SC1 and SC2 suppress *C. difficile*-associated disease in the <sup>Hmb</sup> mouse model. (A) Overview of infection and recurrence protocol used to evaluate simplified communities and FMT treatments. Mice were treated with a mixture of five antibiotics (+5 Abx) in the drinking water for 6 days as described previously (42). After 2 days on fresh water, mice were treated once daily with microbial communities as indicated in panels B to E or with a vehicle (PBS) for 3 days. One day prior to *C. difficile* infection, clindamycin was administered intraperitoneally (Clinda IP). On the third day of administration of microbial communities, mice were challenged with *C. difficile* (Cdiff). Disease severity and levels of *C. difficile* were monitored during initial infection and following induction of relapse with intraperitoneal injection of clindamycin. In panels B to E, treatments are indicated as follows: PBS, dark blue ( $n = 9$ ); <sup>Hmb</sup> mouse FMT (M-FMT), magenta ( $n = 9$ ); human FMT (H-FMT), teal ( $n = 9$ ); SC1, dark purple ( $n = 9$ ); SC2, light blue ( $n = 9$ ); SC3, violet ( $n = 9$ ); and SC4, black ( $n = 8$ ). (B) Percentage of day -2 body mass on day 0 (prior to *C. difficile* challenge) following 2 days of treatment with simplified communities. (C) Percentage of day 0 body mass on day 2 following initial infection (D) Percentage of relapse day 0 body mass 2 days following relapse. (E) Levels of *C. difficile* measured in the feces of treated mice on days indicated below the graph. Boxes represent the interquartile ranges, horizontal lines indicate the medians, and vertical lines indicate the ranges of data collected from replicate mouse samples at each time point. Significance of differences between microbe- and PBS-treated mice in each panel were evaluated with one-way Kruskal-Wallis testing with Dunn's correction for multiple comparisons. *P* values less than 0.05 are reported. Two mice lost from PBS (days 3 and 4) and <sup>Hmb</sup> mouse FMT-treated groups (day 3) were included in calculations until death. Mice treated with SC3 were not tested for resistance to recurrent infection. *C. difficile* levels in H-FMT-treated mice were not tested on relapse day 10. Longitudinal data collected during initial infection and relapse are plotted in Fig. S2.

microbial diversity decreased (Fig. 4C) and species evenness increased (Fig. 4D) with increasing levels of dilution. The majority of OTUs lost through dilution were classified in the order *Clostridiales* (Fig. 4E). We selected three final simplified communities (FS2A, FS2B, and FS2C) to test for the ability to inhibit CDAD in <sup>Hmb</sup> mice.

**FS2B and FS2C suppress CDAD in <sup>Hmb</sup> mice.** We used the experimental approach outlined in Fig. 3 to test final simplified communities FS2A, FS2B, and FS2C. As controls, we administered M-FMT, SC2, and PBS. Similar to the findings in our initial study, PBS-treated mice exhibited body mass loss following challenge with *C. difficile* and weight loss was prevented by treatment with M-FMT (Fig. 4F). Treatment with SC2 prevented body mass loss, contrasting with prior results in which SC2 treatment was partially protective. Changes in efficacy could be due to the shifts in microbial composition upon the reculturing of SC2 (Fig. 4E). FS2B- and FS2C-treated mice were also protected from CDAD, whereas mice treated with community FS2A lost body mass at a level similar to that of PBS-treated mice (Fig. 4F).

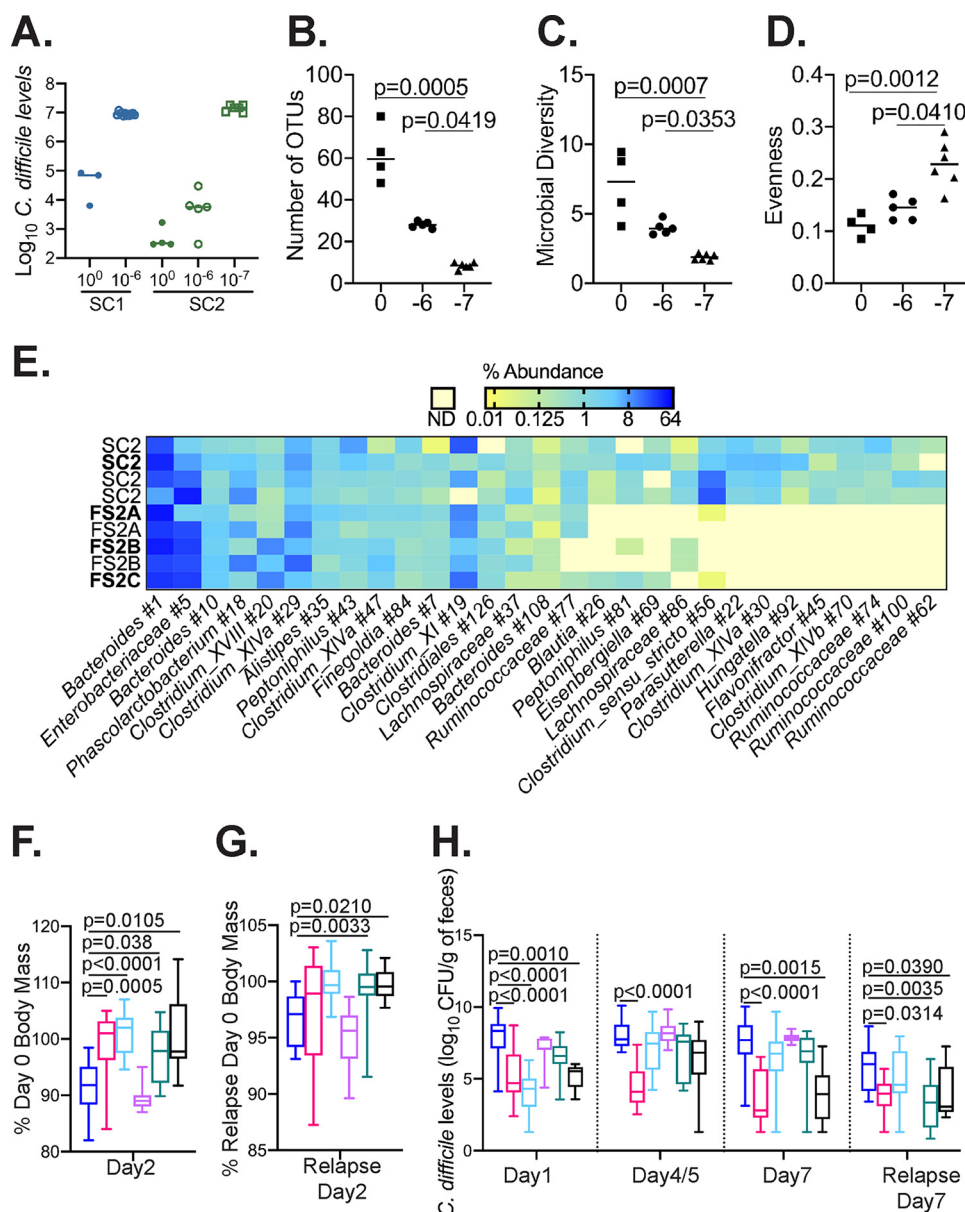


**FIG 4** Identification of final simplified (FS) microbial communities that suppress *C. difficile* in MBRA and  $HMB$  mouse models of CDI. (A) Plot of  $\log_{10}$  *C. difficile* levels on the final day in culture with recultured SC1 (closed blue circles) and SC2 (closed green circles) and in recultured SC1 and SC2 that were further simplified to  $10^{-6}$ -fold (open circles) and  $10^{-7}$ -fold (open squares). Lines represent medians. (B to D) Number of OTUs (B), microbial diversity (inverse Simpson index) (C), and species evenness (Simpson evenness index) (D) of recultured SC2 and communities diluted  $10^{-6}$  and  $10^{-7}$ . Lines represent medians; any significant differences ( $P < 0.05$ ) detected in distributions of communities as determined by one-way Kruskal-Wallis testing are reported. (E) Differences in abundance of OTUs present above 0.1% of total sequences in at least two replicate SC2, FS2A, FS2B, or FS2C cultures. Samples are indicated to the left of the plot; data in boldface type are from the cultures shown in panel A; the first SC2 replicate is from the data reported in Fig. 2, and the additional SC2, FS2A, and FS2B replicates were collected from bioreactor cultures used to gavage  $HMB$  mice in panels F to H. Yellow represents  $<0.01\%$  abundance and blue represents  $>64\%$  of total sequences as indicated by shading of  $\log_2$ -transformed relative abundance data; pale yellow indicates that no sequences were detected (ND). In panels F to H, data were collected from  $HMB$  mice subjected to treatment indicated as follows: PBS, dark blue ( $n = 18$ ); M-FMT, magenta ( $n = 17$ ); SC2, light blue ( $n = 17$ ); FS2A, violet ( $n = 9$ ); FS2B, teal ( $n = 17$ ); and FS2C, black ( $n = 8$ ). Treatments were administered as described for Fig. 3A. (F) Percentage of day 0 body mass on day 2 of infection. (G) Percentage of relapse day 0 body mass on day 2 of relapse. (H)  $\log_{10}$  levels of *C. difficile* in mouse feces on days indicated. Boxes represent the interquartile ranges, horizontal lines indicate the medians, and vertical lines indicate the ranges of data collected from replicate mouse samples at each time point. Significant differences ( $P < 0.05$ ) in distributions of community-treated mice compared to PBS-treated mice as determined by one-way Kruskal-Wallis testing with Dunn's correction for multiple comparisons are reported. Longitudinal data from treatments shown in panels F to H are reported in Fig. S3.



PBS-treated mice shed *C. difficile* in feces at similarly high levels across all time points tested (Fig. 4H). In FS2C-treated mice, *C. difficile* levels were significantly lower than in PBS-treated mice on day 1 and day 7 of infection. In SC2-treated mice, *C. difficile* levels were significantly lower than in PBS-treated mice only on day 1 of infection. FS2A- and FS2B-treated mice showed little reduction in levels of *C. difficile* shedding. M-FMT-treated mice had significantly lower levels of *C. difficile* than PBS-treated mice at all time points.

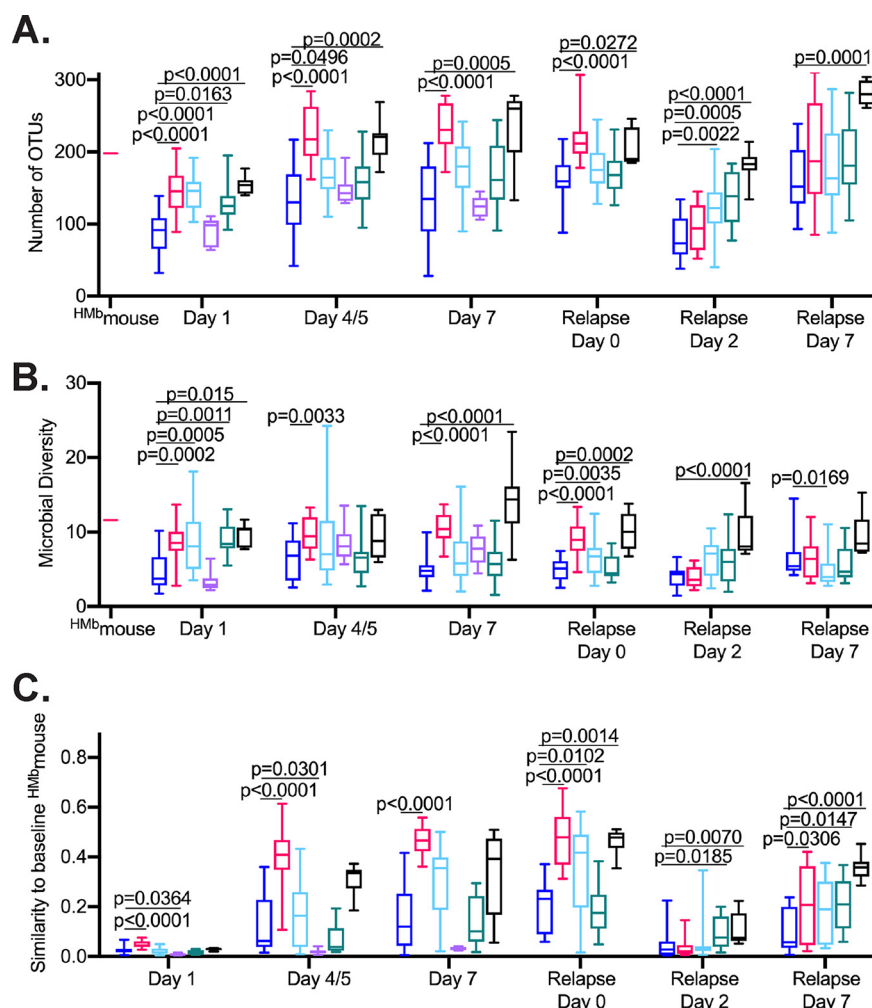
Following induction of relapse, we observed an ~3% median reduction in body mass in PBS-treated mice on day 2 following i.p. injection (Fig. 4G). Mice treated with SC2, FS2B, or FS2C showed <0.5% median body mass loss, whereas FS2A-treated mice exhibited ~5% median body mass loss. M-FMT-treated mice exhibited ~1% decrease in body mass. We also observed more rapid clearance of *C. difficile* in FS2B- and FS2C-treated mice (Fig. 4H).

**Treatment with simplified communities has persistent effects on the fecal microbiome.** We analyzed microbial communities from mouse fecal samples on days 1, 4 or 5, and 7 and relapse days 0, 2, and 7. Sequence data obtained from mice were pooled with bioreactor data to facilitate tracking of bacteria present in simplified communities in treated mice. We found that sequences that clustered at >99% average nucleotide identity (ANI) (Table S2) provided greater resolution of OTUs distinct to *in vitro*-cultured simplified communities and M-FMT-treated <sup>HMB</sup>mice than sequences that clustered at >97% ANI (Table S3). With sequences clustered at >99% ANI, 90% of OTUs found in M-FMT-treated <sup>HMB</sup>mice were not detected in *in vitro* cultures and likely represent indigenous bacteria. Similarly, 81% of OTUs found in *in vitro* cultures were not detected in FMT-treated <sup>HMB</sup>mice. Subsequent analyses used OTUs that clustered at >99% ANI.

The number of OTUs detected on day 1 following infection were 25 to 50% lower across all treatment groups than those observed in the FMT sample collected from mice not treated with antibiotics (Fig. 5A, <sup>HMB</sup>mouse). Treatment with M-FMT partially restored OTU abundance and microbial diversity on day 1; full recovery to levels observed in untreated mice was not observed until day 4 or 5 during infection. In PBS-treated mice, the median number of OTUs detected in fecal samples increased over time but did not return to the levels detected in untreated mice. Treatment with SC2, FS2C, or FS2B significantly increased the number of OTUs detected on day 1 compared to that in PBS-treated mice. Later increases in OTU abundance in FS2C-treated mice paralleled findings for FMT-treated mice. For SC2- and FS2B-treated mice, OTU abundance increased over time but not to the extent observed in FMT-treated mice. Neither OTU abundance nor microbial diversity was significantly different between FS2A-treated and PBS-treated mice over the first week of infection. Treatment with FMT, SC2, FS2B, and FS2C also significantly increased microbial diversity compared to that in PBS-treated mice (Fig. 5B).

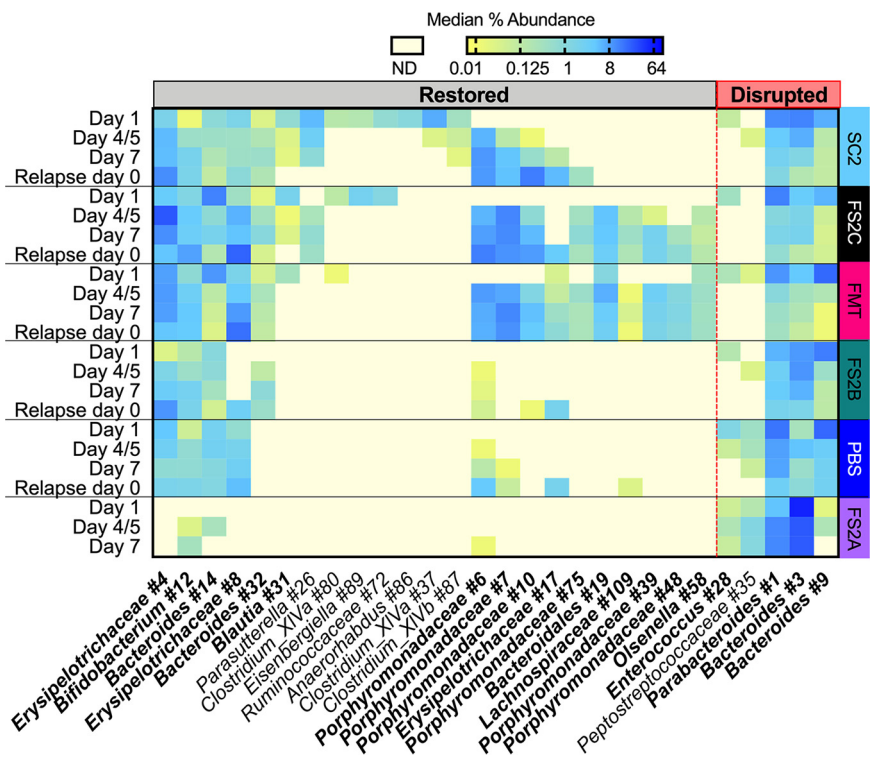
Similarities in community composition between the baseline <sup>HMB</sup>mouse sample not treated with antibiotics and communities in the feces of treated mice were calculated (Fig. 5C). In M-FMT-treated mice, fecal communities had low similarities to the baseline <sup>HMB</sup>mouse sample on day 1, but similarities increased by day 7 (Fig. 5C). In contrast, similarities between PBS-treated mice and the baseline untreated <sup>HMB</sup>mouse sample were significantly lower than M-FMT-treated mice through relapse day 0. Compared to PBS-treated mice, FS2C- and SC2-treated mice exhibited an accelerated return toward the baseline microbiome composition. FS2B-treated mice exhibited a return to baseline microbiome that paralleled that in PBS-treated mice. In contrast, FS2A-treated mice exhibited significantly reduced recovery of microbiome composition compared to that of PBS-treated mice, indicating that FS2A treatment may suppress recovery of the fecal microbiome.

**Treatments shift the composition of indigenous bacteria.** We identified 98 OTUs that were significantly enriched or depleted in treatments that accelerated microbiome recovery (FMT, FS2C, and SC2) compared to treatments with more prolonged disrup-



**FIG 5** Treatment with SC2 and FS2C restores microbial diversity and shifts microbiome composition toward baseline state observed in <sup>Hmb</sup>mice not treated with antibiotics. 16S rRNA gene sequence data were obtained from bacteria present in the feces of mice treated with PBS (dark blue), M-FMT (magenta), SC2 (light blue), FS2A (violet), FS2B (teal), or FS2C (black) on days 1, 4 or 5, and 7 following initial *C. difficile* infection and days 0, 2, and 7 relative to initiation of relapse with clindamycin i.p. (For FS2A-treated mice, 16S rRNA gene sequence data were obtained only from samples collected during initial infection for FS2A-treated mice.) 16S rRNA sequence data were also obtained from a pooled fecal sample collected from an <sup>Hmb</sup>mice not treated with antibiotics that was used for FMT administration. (A and B) Number of OTUs (A) and microbial diversity (inverse Simpson index) (B) measured in sample collected from <sup>Hmb</sup>mice not treated with antibiotics used for FMT administration (<sup>Hmb</sup>mouse) and in samples collected from treated mice at time points indicated below the graph. (C) Similarity to baseline <sup>Hmb</sup>mouse sample used for FMT administration measured in samples at time points indicated below graph (similarity = 1 – Bray-Curtis dissimilarity). Boxes represent the interquartile ranges, horizontal lines indicate the medians, and vertical lines indicate the ranges of data collected from replicate mouse samples at each time point. Significance of differences in microbe-treated compared to PBS-treated animals at each time point were evaluated with one-way Kruskal-Wallis testing with Dunn's correction for multiple comparisons; *P* values of <0.05 are reported.

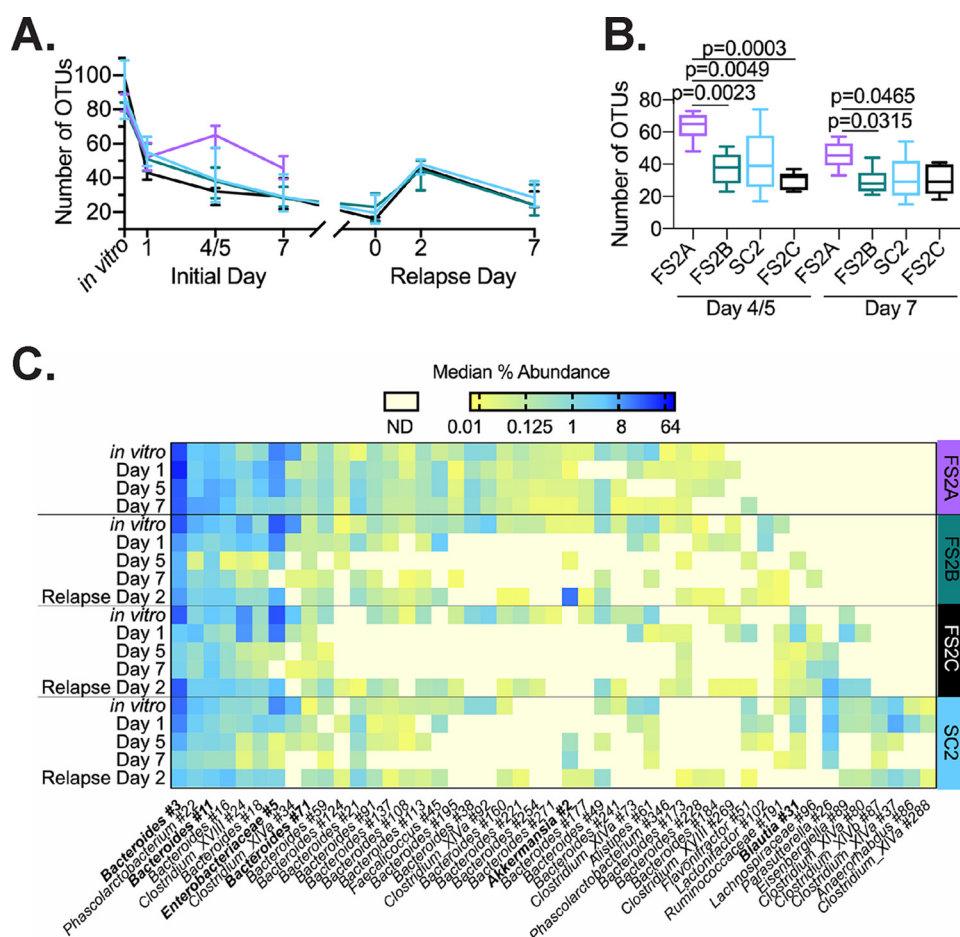
tion (PBS, FS2A, and FS2B) for at least one of the time points tested (Table S3). We focused on OTUs with the largest predicted effect sizes (linear discriminant analysis [LDA] > 3 [Fig. 6]). Three OTUs, *Erysipelotrichaceae* number 4, *Bifidobacterium* number 12, and *Bacteroidales* number 19, were significantly enriched in FS2C-, SC2-, and FMT-treated mice at all time points. *Erysipelotrichaceae* number 8, *Blautia* number 31, and *Clostridium* XIVa number 80 were enriched in FS2C-, SC2-, and FMT-treated mice on day 1, whereas several *Porphyromonadaceae* OTUs (numbers 6, 7, 10, 75, 39, and 48) as well as three *Firmicutes* OTUs (*Erysipelotrichaceae* number 17, *Lachnospiraceae* number 109, and *Olsenella* number 48) were enriched in FS2C-, SC2-, and FMT-treated mice at



**FIG 6** Treatment with simplified communities alters recovery of indigenous microbes. We used linear discriminant analysis effect size (LEfSe) to identify significantly enriched or depleted taxa between treatments that accelerated microbiome recovery in Fig. 5C (M-FMT, FS2C, and SC2 [Restored]) and treatments with more prolonged disruption (PBS, FS2A, and FS2B [Disrupted]). Independent analyses were performed for samples on days 1, 4 or 5, and 7 and relapse day 0; OTUs with LDA values determined by LEfSe of  $>3$  for at least one time point are shown. Intensity of shading correlates to the  $\log_2$ -transformed median percent abundance measured for the treated mice at the indicated time points, with median abundances of  $>64\%$  shaded dark blue and median values equal to  $0.01\%$  shaded dark yellow. Samples in which sequences were below the detection limit (ND, not detected) are shaded pale yellow. OTUs in bold typeface are indigenous to <sup>HMb</sup>mice as described in Table S2. OTUs in standard typeface were found only in simplified communities. *Blautia* number 31 and *Bacteroides* number 3 were found in both <sup>HMb</sup>mice and simplified communities. *Peptostreptococcaceae* number 35 is likely *C. difficile*, as the representative sequence has 100% identity to *C. difficile* and abundance over the course of infection correlates well with *C. difficile* levels reported in Fig. 3 and 4. The complete set of OTUs identified by LEfSe is provided in Table S4.

later time points. On day 1 of infection, *Peptostreptococcaceae* number 35 and *Enterococcus* number 28 were enriched in the feces of PBS-, FS2A-, and FS2B-treated mice, whereas *Bacteroides* number 3, *Bacteroides* number 9, and *Parabacteroides* number 1 were enriched during the later stages of infection. These results demonstrate that return toward the baseline microbiome configuration correlates with restoration of members of multiple phyla (*Bacteroidetes*, *Firmicutes*, and *Actinobacteria*), whereas continued disruption correlates with increased abundance of *Bacteroides* OTUs and a *Peptostreptococcaceae* OTU that is likely *C. difficile*.

**Bacteria from simplified communities persist in the feces of treated mice.** We tracked the fate of OTUs present in *in vitro*-cultured simplified communities over time in mice treated with simplified communities. On day 1 following infection,  $\sim 60\%$  of OTUs present in *in vitro*-cultured simplified communities could be detected in the feces of treated mice (Fig. 7A; median OTU levels ranged from 43 to 55 OTUs). Levels of simplified community OTUs decreased over time, with the lowest number of OTUs (16 to 23) detected on relapse day 0 (Fig. 7A). Following induction of relapse, the number of OTUs detected from the original *in vitro*-cultured simplified communities increased to 44 to 48. These results indicate that these OTUs had likely persisted below the level of detection and reemerged when other OTUs declined following clindamycin treat-



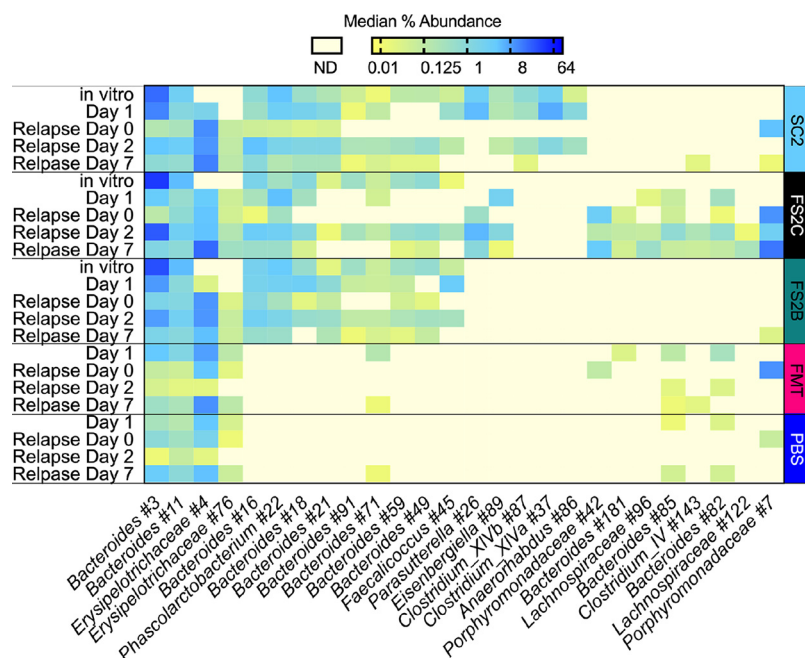


**FIG 8** Treatment with SC2, FS2C and FS2B led to distinct microbiome responses during disease relapse. LEfSe was used to identify OTUs that differed significantly between treatment groups in the feces of mice on days 2 and 7 following induction of relapse with clindamycin i.p. Independent analyses were performed for samples on relapse days 2 and 7; OTUs with LDA values determined by LEfSe of  $>3$  for at least one time point are shown. The complete set of LEfSe data is shown in Table S6. Median abundance of OTUs in *in vitro* SC2, FS2C, and FS2B cultures as well as all the feces of treated mice on day 1 and relapse day 0 samples are included for comparison as described in the text.

groups during relapse and identified 26 OTUs that showed high levels of difference between treatment groups during relapse. Approximately 70% of these OTUs enriched in the feces of SC2-, FS2C-, and FS2B-treated mice on relapse day 2 likely originated from the *in vitro*-cultured simplified communities (Fig. 8). Approximately 20% of OTUs enriched on relapse day 2 were enriched on day 1 of infection, indicating that the response to relapse was not identical to the initial disruption but shared some similarities. Similar to the kinetics observed during initial infection (Fig. 6), 11 of 26 OTUs were also significantly enriched on relapse day 7, while the remainder had decreased in abundance.

## DISCUSSION

We described a new pipeline for identifying and rigorously testing simplified communities with the ability to protect against *C. difficile* infection. We identified 24 new simplified communities with the ability to inhibit *C. difficile in vitro*. Several of the OTUs detected in these simplified communities were classified into families (*Lachnospiraceae*, *Ruminococcaceae*, *Clostridiaceae*, and *Bacteroidaceae*) and genera (*Bacteroides*, *Clostridium* XIVa, *Anaerostipes*, *Coprococcus*, *Dorea*, *Roseburia*, and *Blautia*) found depleted in the fecal microbiomes of people who are susceptible to *C. difficile* and restored following FMT treatment (43–47). In contrast, some OTUs were classified into families less often linked to resistance to *C. difficile* colonization (e.g., *Veillonella*, *Eggerthella*, *Clostridium* XVIII, and *Acidaminococcus*) or more correlated with susceptibility to *C. difficile* infection (*Enterococcus*, *Streptococcus*, and *Escherichia/Shigella*). Thus, the approach we described leads to communities distinct from those based upon predictive ecological modeling and may provide additional insights into *C. difficile* colonization resistance.

By testing simplified communities in an <sup>HMb</sup>mouse model, we determined that only a subset of the tested communities conferred protection *in vivo*. Treatment with one community, SC4, resulted in loss of body mass consistent with toxicity of one or more



members of this community. Although it is not clear which community member(s) in SC4 are toxic, SC4 contains a *Bilophila* OTU that could be the source of toxicity; treatment of specific-pathogen-free (SPF) mice with *Bilophila wadsworthia* caused weight loss as a result of systemic inflammation (48). Treatment with SC1, SC2, FS2B, and FS2C significantly reduced the initial body mass loss associated with severe disease and decreased *C. difficile* loads early in infection, similar to treatment with <sup>HMB</sup>mouse FMT (M-FMT). While the magnitudes of effects varied, we observed a significant negative correlation between *C. difficile* levels on day 1 of infection and body mass on day 2 of infection (Fig. S4), with lower levels of *C. difficile* on day 1 predictive of reduced body mass loss on day 2 of infection. Thus, a potential mechanism for simplified communities to limit the severity of CDI *in vivo* is by delaying the germination or outgrowth of *C. difficile* spores. Similar reductions in *C. difficile* levels on day 1 following infection coupled to an ~50% reduction in body mass loss were reported by Buffie et al. (22) when mice were treated with a consortium of four strains. In this case, early reductions in *C. difficile* levels were linked with restoration of secondary bile acid production by *Clostridium scindens*, as well as unknown functions contributed by other members of the simple community. Delaying germination or outgrowth could prevent severe disease by altering the dynamics of the host immune response between proinflammatory responses known to cause disease and anti-inflammatory responses that provide protection from *C. difficile* epithelial damage (21, 49, 50).

Comparison of microbiome changes in the feces of mice treated with communities that limit (FS2C, SC2, and M-FMT), partially limit (FS2B), or fail to limit (FS2A and PBS) CDAD may explain some of the observed differences in disease progression. Treatment with FS2C, SC2, or M-FMT significantly limited body mass loss and altered the levels of *C. difficile* shedding; these communities also exhibited a more rapid return toward the baseline microbiome configuration observed in <sup>HMB</sup>mice not treated with antibiotics. Return toward baseline was associated with an increased abundance of members of the indigenous microbiome, including several *Porphyromonadaceae* OTUs. *Porphyromonadaceae* were found to be depleted in the feces of humans and mice susceptible to *C. difficile* (51, 52). Enhanced restoration of indigenous microbes observed in FS2C- and SC2-treated mice could be due to the restoration of syntrophic interactions between indigenous microbes and those found in simplified communities and/or suppression of factors (i.e., *C. difficile* metabolism [53] and innate immune activation [54]) that promote microbiome disruption.

Mice treated with FS2B showed limited body mass loss during initial infection but did not show significantly altered *C. difficile* shedding in feces and exhibited a slower return to baseline microbiome conditions. A return to baseline microbiome conditions could, therefore, be important for *C. difficile* clearance but may not be required to mitigate initial disease severity. Treatment with FS2A, which failed to provide protection *in vivo*, was associated with significantly lower levels of restoration of indigenous microbes. Previous reports have indicated that specific probiotic formulations can delay the return to a nondisrupted microbiome configuration due to suppression of indigenous microbes (55); this could also be true for FS2A-treated mice. Further studies are needed to evaluate these hypotheses.

A subset of OTUs that originated from simplified communities persisted over time in the feces of treated mice. While the abundance of these OTUs diminished over time, continued colonization was demonstrated following induction of relapse. Persistence of these simplified community OTUs likely played a key role in limiting susceptibility to recurrent disease. One OTU of note was *Phascolarctobacterium*. A recent study demonstrated that administration of *Phascolarctobacterium* species to cefoperazone-treated mice reduces mortality, possibly by competing with *C. difficile* for succinate in the disrupted gastrointestinal (GI) tract (56). Other OTUs of note include those classified as *Blautia*, *Ruminococcaceae*, and *Eisenbergiella*. Colonization with members of the *Ruminococcaceae* family and the *Eisenbergiella* and *Blautia* genera was correlated with a 60% reduced risk for CDI in allogeneic hematopoietic stem cell patients (57). Our results are also consistent with a previous study of microbiome restoration following FMT in

human patients that found a balance between engraftment of donor bacteria, persistence of bacteria present in the feces of infected patients, and emergence of previously undetected bacteria (58).

Dilution-extinction provided a rapid way to screen simplified communities for the ability to prevent *C. difficile* infection. Development of diverse treatment consortia for CDI is important, as *C. difficile* is known to fill different nutritional niches (59) and fecal transplant studies indicate differential engraftment of species between patients treated with the same fecal sample (60). However, further refinement is needed before communities progress to clinical testing. Isolation of individual strains from simplified communities prior to community reassembly and efficacy testing will ensure the identity of the treatment consortia. In spite of these limitations, the approaches outlined in this report represent a significant advance in the throughput of testing for simplified communities to limit *C. difficile* infection and could potentially be adapted to identify simplified communities to treat other diseases linked to microbiome disruption.

## MATERIALS AND METHODS

**Fecal samples, bacterial strains, and cultivation conditions.** Fecal samples were provided by anonymous subjects between the ages of 25 and 64 years who self-identified as healthy and had not consumed antibiotics for at least 2 months or probiotics for at least 2 days prior to donation. Fecal samples were prepared as described previously (61). The previously described ribotype 027 isolate *C. difficile* 2015 was used for all experiments (61). All cultivation was performed at 37°C under an atmosphere of 5% H<sub>2</sub>, 5% CO<sub>2</sub>, and 90% N<sub>2</sub>.

**Identification of simplified communities through dilution/extinction.** Fecal samples were prepared and inoculated into MBRAs containing bioreactor medium 3 (BRM3) (62) as described previously (40). Briefly, frozen fecal aliquots were thawed and used to prepare 25% (wt/vol) fecal slurries in PBS under anaerobic conditions. After being vortexed for 5 min, the slurries were briefly centrifuged (5 min, 201 × g), and clarified supernatants were used to inoculate the reactors. Fecal communities were equilibrated for 16 h in batch growth before initiation of continuous flow (flow rate of 1.875 ml/h; 8-h retention time). After 5 to 6 days, an aliquot was removed for determination of cell concentration through serial dilution and plating on BRM3 agar and determination of *C. difficile* colonization status by PCR as described below. (Analysis was limited to D2 to D4 and D6 communities; D1 and D5 communities were not tested.) After 8 days, a sample was removed from each reactor and diluted to a final concentration of  $\sim 3 \times 10^4$  cells/ml ( $10^{-4}$  dilution) or  $3 \times 10^3$  cells/ml ( $10^{-5}$  dilution) in BRM3. One milliliter of each dilution was used to inoculate 5 or 6 sterile bioreactors containing 15 ml of sterile BRM3/dilution. After 3 days under continuous flow, aliquots were removed from diluted communities for sequencing and for cryopreservation with 15% glycerol or 7.5% dimethyl sulfoxide (DMSO). One day later, communities were challenged with  $10^4$  *C. difficile* cells as described previously (61); *C. difficile* levels in reactors were determined through selective plating on TCFA agar with 20 µg/ml of erythromycin and 50 µg/ml of rifampin as described previously (61). For repeat cultivation, cryopreserved stocks were thawed and 300 µl was used to inoculate triplicate reactor vessels containing 15 ml of sterile BRM3. Communities were grown in batch for 16 h and then with continuous flow for 4 days prior to challenge with *C. difficile* as described above.

**Analysis of *C. difficile* colonization status in undiluted communities D2, D3, D4, and D6.** As described above, 1-ml samples were removed from undiluted cultures on day 5 of cultivation. Cells were concentrated by centrifugation at  $\sim 20,000 \times g$  for 1 min. The supernatant was discarded and cells were lysed by bead-beating in sterile water as previously described (40). One microliter of cell lysate was used as the template in PCRs to detect *C. difficile tcdA* or bacterial 16S rRNA (broad-range 16S rRNA primers) using previously described primers (61) added at a final concentration of 1 µM to reaction mixtures containing Denville Taq master mix otherwise formulated according to the manufacturer's instructions. After 35 cycles of amplification (94°C for 45 s, 55°C for 30 s, and 72°C for 1 min), 10-µl volumes of products were analyzed by agarose gel electrophoresis. Undiluted cultures had positive signals for the 16S rRNA gene as expected and no signal for *C. difficile tcdA*.

**Further simplification of SC1 and SC2.** One-milliliter stocks were thawed and used to inoculate an empty reactor vessel. The flow of sterile BRM3 was initiated and allowed to fill the reactor at a flow rate of 1.825 ml/h. After 3 days, cell concentrations were determined as described above. Two days later, aliquots of cells were removed and diluted in sterile BRM3 to a final concentration of 250 cells/ml ( $10^{-6}$  dilution) or 25 cells/ml ( $10^{-7}$  dilution). One-milliliter aliquots of cells were used to inoculate 5 ( $10^{-6}$  dilution) or 6 ( $10^{-7}$  dilution) empty, sterile reactors, which were allowed to fill with sterile medium as described above. After 2 (SC2) or 3 (SC1) days of flow, aliquots were removed for sequence analysis and cryopreservation. One (SC1) or 15 (SC2) days later, simplified communities were challenged with  $10^4$  vegetatively growing *C. difficile* cells and levels of *C. difficile* persisting in reactors over time were determined through selective plating.

**Cultivation of simple communities for the treatment of HMB mice.** Bioreactors (65 ml) were prepared as previously described (63). Sterile, empty bioreactors were inoculated with 1 ml of thawed stocks and allowed to fill with sterile BRM3 at a flow rate of 8.125 ml/h. Communities were cultured with flow for 6 to 8 days before 10-ml aliquots of culture were removed, centrifuged ( $800 \times g$  for 10 min), and

resuspended in 1-ml anaerobic PBS for delivery to mice. Cell densities of reactor communities were determined through selective plating on BRM3 agar; mice received doses ranging from  $5 \times 10^8$  to  $2 \times 10^9$  cells freshly prepared from reactors on three subsequent days.

**Preparation of <sup>HMB</sup>mouse FMT and human FMT material.** Fecal samples were collected from 6- to 10 week-old male and female <sup>HMB</sup>mice (42), pooled, and resuspended in anaerobic PBS at 20% (wt/vol). Samples were vortexed for 5 min and then centrifuged at  $200 \times g$  for 2 min. Each mouse was treated with 100  $\mu$ l of clarified fecal slurry. The human FMT preparation was prepared as described previously (64).

**Treatment of <sup>HMB</sup>mice with PBS, human FMT, <sup>HMB</sup>mouse FMT, or simplified communities.** Antibiotics (61) were administered in the drinking water to 6- to 10-week-old male and female mice (Fig. 3A). Mice were treated with 100  $\mu$ l of PBS, <sup>HMB</sup>mouse FMT (M-FMT), human FMT (H-FMT), or cells from simplified communities via orogastric gavage on three subsequent days. Clindamycin (10 mg/kg of body weight) was administered via intraperitoneal injection. Mice were challenged with  $5 \times 10^4$  spores of *C. difficile* 2015. Three mouse experiments were performed. Mice in experiment 1 were treated with PBS, M-FMT, H-FMT, or SC1 to SC4 ( $n = 9$  mice/treatment group except SC4 [ $n = 8$ ]). Mice in experiment 2 were treated with PBS, M-FMT or SC2, FS2A, or FS2B ( $n = 9$  mice/treatment group except PBS [ $n = 10$ ]). Mice in experiment 3 were treated with PBS, M-FMT or SC2, FS2B, or FS2C ( $n = 8$  mice/treatment group). In experiments 1 and 2,  $\sim 100 \mu$ l of inoculum from the 3rd treatment was saved for sequencing. Mouse body mass was collected daily from days 0 to 5 following *C. difficile* challenge and then periodically following resolution of severe disease as indicated in figures. Mice that lost greater than 20% body mass from day 0 or showed signs of severe disease as previously described (42) were euthanized. Mouse body mass was also collected on day  $-2$  and day  $-1$  in experiment 1. Relapse was induced 24 (experiment 3), 28 (experiment 1), or 33 (experiment 2) days following initial *C. difficile* infection through i.p. administration of clindamycin (10 mg/kg). *C. difficile* levels in fecal samples were determined through selective plating (experiment 1) or qPCR (experiments 2 and 3) as described previously (61) at the time points indicated.

**Analysis of microbial communities through 16S rRNA gene sequencing.** Nucleic acids were extracted from mouse fecal samples and inoculum samples using the DNeasy Powersoil HTP kit (Qiagen) and from the further-simplified SC2 samples using the Powermag microbiome kit (MoBio). The V4 region of the 16S rRNA gene was amplified from purified DNA or directly from lysed bioreactor samples in triplicate using dual or single indexed primers F515/R806 as described previously (40, 65). Samples were cleaned quantified and pooled in equimolar concentrations prior to sequencing using the Illumina MiSeq v2  $2 \times 250$  kit as described previously (40).

All sequence analysis was performed using mothur version 1.35.1. Raw sequencing reads were quality filtered, aligned to the V4 region of Silva 16S rRNA reference release 132, preclustered into sequence groups with  $<1\%$  sequence divergence, filtered to remove chimeras with uchime, and classified with the Bayesian classifier using rdp database version 16 ( $>80\%$  confidence threshold) as previously described, with the modifications noted above (40, 66). Sequence data were then rarefied to remove those sequences with  $<10$  reads. Pairwise distance matrices were calculated and sequences were clustered into OTUs with  $>97$  and  $>99\%$  ANI. OTUs were classified by the majority consensus rdp taxonomy within the OTU. To better determine the potential identity of *Peptostreptococcaceae* OTU number 31 ( $>97\%$  ANI) and *Peptostreptococcaceae* OTU number 35 ( $>99\%$  ANI), representative sequences from these OTUs were compared to the nr/nt database using BLAST.

Samples were randomly subsampled to 10,000 sequences before determination of alpha and beta diversity measures. Alpha diversity measures (number of observed OTUs, inverse Simpson diversity, and Simpson evenness) were calculated using mothur. Principal-coordinate analysis of Bray-Curtis dissimilarities between communities were calculated and ordinates were visualized using the Phyloseq package (version 1.30.0 [67]) running in R version 3.61. Simplified communities were partitioned into four community types with Dirichlet multinomial mixtures as implemented in mothur version 1.44.0. Identification of OTUs significantly enriched between treatment groups in mouse experiments was performed using the mothur implementation of LEfSe (40, 66). mothur was also used to calculate the Bray-Curtis dissimilarities between treated mice and the baseline <sup>HMB</sup>mouse sample (similarity =  $1 - \text{Bray-Curtis dissimilarity}$ ).

**Ethics statement.** Protocols for fecal sample collection were reviewed and approved by the Institutional Review Boards of Michigan State University and Baylor College of Medicine. Animal use was reviewed and approved by the Institutional Animal Care and Use Committee at Baylor College of Medicine (protocol number AN-6675).

**Data visualization and statistical analysis.** Unless otherwise noted, data were visualized and statistical analysis was performed using Prism v8.

**Data availability.** 16S rRNA gene sequence data have been deposited in the Sequence Read Archive with accession number [PRJNA632592](https://www.ncbi.nlm.nih.gov/sra/PRJNA632592).

## SUPPLEMENTAL MATERIAL

Supplemental material is available online only.

**FIG S1**, PDF file, 0.4 MB.

**FIG S2**, PDF file, 1.7 MB.

**FIG S3**, PDF file, 1.2 MB.

**FIG S4**, PDF file, 0.5 MB.

**TABLE S1**, XLSX file, 0.04 MB.

**TABLE S2**, XLSX file, 0.03 MB.

**TABLE S3**, XLSX file, 0.02 MB.

**TABLE S4**, XLSX file, 0.04 MB.

**TABLE S5**, XLSX file, 0.03 MB.

**TABLE S6**, XLSX file, 0.1 MB.

## ACKNOWLEDGMENTS

This work was supported by funding from the National Institutes of Allergy and Infectious Disease (AI12152201 and AI123278) to R.A.B. and from the Nebraska Tobacco Settlement Biomedical Research Development Fund to J.M.A. Analysis was completed utilizing the Holland Computing Center, which receives support from the Nebraska Research Initiative. R.A.B. receives unrestricted research support from BioGaia, AB, consults for Takeda and Probiotech, serves on the scientific advisory board of Tenza, and is a cofounder of Mikroviva.

We thank T. Savidge (Texas Children's Microbiome Center, Baylor College of Medicine) for providing the human FMT sample.

## REFERENCES

1. Lessa FC, Winston LG, McDonald LC, Emerging Infections Program C. *difficile* Surveillance Team. 2015. Burden of *Clostridium difficile* infection in the United States. *N Engl J Med* 372:2369–2370. <https://doi.org/10.1056/NEJMc1505190>.
2. Miller BA, Chen LF, Sexton DJ, Anderson DJ. 2011. Comparison of the burdens of hospital-onset, healthcare facility-associated *Clostridium difficile* infection and of healthcare-associated infection due to methicillin-resistant *Staphylococcus aureus* in community hospitals. *Infect Control Hosp Epidemiol* 32:387–390. <https://doi.org/10.1086/659156>.
3. Wiström J, Norrby SR, Myhre EB, Eriksson S, Granström G, Lagergren L, Englund G, Nord CE, Svenungsson B. 2001. Frequency of antibiotic-associated diarrhoea in 2462 antibiotic-treated hospitalized patients: a prospective study. *J Antimicrob Chemother* 47:43–50. <https://doi.org/10.1093/jac/47.1.43>.
4. Dubberke ER, Olsen MA. 2012. Burden of *Clostridium difficile* on the healthcare system. *Clin Infect Dis* 55:S88–S92. <https://doi.org/10.1093/cid/cis335>.
5. Bagdasarian N, Rao K, Malani PN. 2015. Diagnosis and treatment of *Clostridium difficile* in adults: a systematic review. *JAMA* 313:398–408. <https://doi.org/10.1001/jama.2014.17103>.
6. Johnson S. 2009. Recurrent *Clostridium difficile* infection: a review of risk factors, treatments, and outcomes. *J Infect* 58:403–410. <https://doi.org/10.1016/j.jinf.2009.03.010>.
7. Wilcox MH, Ahir H, Coia JE, Dodgson A, Hopkins S, Llewelyn MJ, Settle C, McLain-Smith S, Marcella SW. 2017. Impact of recurrent *Clostridium difficile* infection: hospitalization and patient quality of life. *J Antimicrob Chemother* 72:2647–2656. <https://doi.org/10.1093/jac/dkx174>.
8. Shah DN, Aitken SL, Barragan LF, Bozorgui S, Goddu S, Navarro ME, Xie Y, DuPont HL, Garey KW. 2016. Economic burden of primary compared with recurrent *Clostridium difficile* infection in hospitalized patients: a prospective cohort study. *J Hosp Infect* 93:286–289. <https://doi.org/10.1016/j.jhin.2016.04.004>.
9. Sorg JA, Sonenshein AL. 2008. Bile salts and glycine as cogerminants for *Clostridium difficile* spores. *J Bacteriol* 190:2505–2512. <https://doi.org/10.1128/JB.01765-07>.
10. Howerton A, Ramirez N, Abel-Santos E. 2011. Mapping interactions between germinants and *Clostridium difficile* spores. *J Bacteriol* 193:274–282. <https://doi.org/10.1128/JB.00980-10>.
11. Ng KM, Ferreyra JA, Higginbottom SK, Lynch JB, Kashyap PC, Gopinath S, Naidu N, Choudhury B, Weimer BC, Monack DM, Sonnenburg JL. 2013. Microbiota-liberated host sugars facilitate post-antibiotic expansion of enteric pathogens. *Nature* 502:96–99. <https://doi.org/10.1038/nature12503>.
12. Theriot CM, Koenigsnecht MJ, Carlson PE, Hatton GE, Nelson AM, Li B, Huffnagle GB, Z Li J, Young VB. 2014. Antibiotic-induced shifts in the mouse gut microbiome and metabolome increase susceptibility to *Clostridium difficile* infection. *Nat Commun* 5:3114. <https://doi.org/10.1038/ncomms4114>.
13. Wilson KH, Perini F. 1988. Role of competition for nutrients in suppression of *Clostridium difficile* by the colonic microflora. *Infect Immun* 56:2610–2614. <https://doi.org/10.1128/IAI.56.10.2610-2614.1988>.
14. Rolfe RD. 1984. Role of volatile fatty acids in colonization resistance to *Clostridium difficile*. *Infect Immun* 45:185–191. <https://doi.org/10.1128/IAI.45.1.185-191.1984>.
15. May T, Mackie RI, Fahey GC, Cremin JC, Garleb KA. 1994. Effect of fiber source on short-chain fatty acid production and on the growth and toxin production by *Clostridium difficile*. *Scand J Gastroenterol* 29:916–922. <https://doi.org/10.3109/00365529409094863>.
16. Rea MC, Sit CS, Clayton E, O'Connor PM, Whittall RM, Zheng J, Vederas JC, Ross RP, Hill C. 2010. Thuricin CD, a post-translationally modified bacteriocin with a narrow spectrum of activity against *Clostridium difficile*. *Proc Natl Acad Sci U S A* 107:9352–9357. <https://doi.org/10.1073/pnas.0913554107>.
17. Mathur H, Rea MC, Cotter PD, Ross RP, Hill C. 2014. The potential for emerging therapeutic options for *Clostridium difficile* infection. *Gut Microbes* 5:696–710. <https://doi.org/10.4161/19490976.2014.983768>.
18. Rea MC, Dobson A, O'Sullivan O, Crispie F, Fouhy F, Cotter PD, Shanahan F, Kiely B, Hill C, Ross RP. 2011. Effect of broad-and narrow-spectrum antimicrobials on *Clostridium difficile* and microbial diversity in a model of the distal colon. *Proc Natl Acad Sci U S A* 108:4639–4644. <https://doi.org/10.1073/pnas.1001224107>.
19. Péchiné S, Collignon A. 2016. Immune responses induced by *Clostridium difficile*. *Anaerobe* 41:68–78. <https://doi.org/10.1016/j.anaerobe.2016.04.014>.
20. Madan R, Petri WA, Jr. 2012. Immune responses to *Clostridium difficile* infection. *Trends Mol Med* 18:658–666. <https://doi.org/10.1016/j.molmed.2012.09.005>.
21. Saleh MM, Petri WA. 2019. Type 3 immunity during *Clostridioides difficile* infection: too much of a good thing? *Infect Immun* 88:e00306-19. <https://doi.org/10.1128/IAI.00306-19>.
22. Buffie CG, Bucci V, Stein RR, McKenney PT, Ling L, Gobourne A, No D, Liu H, Kinnebrew M, Viale A, Littmann E, van den Brink MRM, Jenq RR, Taur Y, Sander C, Cross JR, Toussaint NC, Xavier JB, Pamer EG. 2015. Precision microbiome reconstitution restores bile acid mediated resistance to *Clostridium difficile*. *Nature* 517:205–208. <https://doi.org/10.1038/nature13828>.
23. Theriot CM, Bowman AA, Young VB. 2016. Antibiotic-induced alterations of the gut microbiota alter secondary bile acid production and allow for *Clostridium difficile* spore germination and outgrowth in the large intestine. *mSphere* 1:e00045-15. <https://doi.org/10.1128/mSphere.00045-15>.
24. Dethlefsen L, Relman DA. 2011. Incomplete recovery and individualized responses of the human distal gut microbiota to repeated antibiotic perturbation. *Proc Natl Acad Sci U S A* 108(Suppl 1):4554–4561. <https://doi.org/10.1073/pnas.1000087107>.
25. Dethlefsen L, Huse S, Sogin ML, Relman DA. 2008. The pervasive effects of an antibiotic on the human gut microbiota, as revealed by deep 16S rRNA sequencing. *PLoS Biol* 6:e280. <https://doi.org/10.1371/journal.pbio.0060280>.



26. Young VB, Schmidt TM. 2004. Antibiotic-associated diarrhea accompanied by large-scale alterations in the composition of the fecal microbiota. *J Clin Microbiol* 42:1203–1206. <https://doi.org/10.1128/jcm.42.3.1203-1206.2004>.
27. Slimings C, Riley TV. 2014. Antibiotics and hospital-acquired *Clostridium difficile* infection: update of systematic review and meta-analysis. *J Antimicrob Chemother* 69:881–891. <https://doi.org/10.1093/jac/dkt477>.
28. Deshpande A, Pasupuleti V, Thota P, Pant C, Rolston DDK, Sfera TJ, Hernandez AV, Donskey CJ. 2013. Community-associated *Clostridium difficile* infection and antibiotics: a meta-analysis. *J Antimicrob Chemother* 68:1951–1961. <https://doi.org/10.1093/jac/dkt129>.
29. Vardakas KZ, Trigkidis KK, Boukouvala E, Falagas ME. 2016. *Clostridium difficile* infection following systemic antibiotic administration in randomised controlled trials: a systematic review and meta-analysis. *Int J Antimicrob Agents* 48:1–10. <https://doi.org/10.1016/j.ijantimicag.2016.03.008>.
30. Brown KA, Khanafer N, Daneman N, Fisman DN. 2013. Meta-analysis of antibiotics and the risk of community-associated *Clostridium difficile* infection. *Antimicrob Agents Chemother* 57:2326–2332. <https://doi.org/10.1128/AAC.02176-12>.
31. Guery PB, Menichetti PFM, Veli-Jukka V-J, Adomakoh NA, Aguado P, Bisnauthsing KB, Georgopali AG, Goldenberg SDG, Karas AK, Kazeem GK, Longshaw CL, Palacios-Fabrega J-F, Cornely P, Vehreschild M, EXTEND Clinical Study Group. 2018. Extended-pulsed fidaxomicin versus vancomycin for *Clostridium difficile* infection in patients 60 years and older (EXTEND): a randomised, controlled, open-label, phase 3b/4 trial. *Lancet Infect Dis* 18:296–307. [https://doi.org/10.1016/S1473-3099\(17\)30751-X](https://doi.org/10.1016/S1473-3099(17)30751-X).
32. Wilcox MH, Gerding DN, Poxton IR, Kelly C, Nathan R, Birch T, Cornely OA, Rahav G, Bouza E, Lee C, Jenkin G, Jensen W, Kim Y-S, Yoshida J, Gabryelski L, Pedley A, Eves K, Tipping R, Guris D, Kartsonis N, Dorr M-B, MODIFY I and MODIFY II Investigators. 2017. Bezlotoxumab for prevention of recurrent *Clostridium difficile* infection. *N Engl J Med* 376:305–317. <https://doi.org/10.1056/NEJMoa1602615>.
33. Jiang ZD, Ajami NJ, Petrosino JF, Jun G, Hanis CL, Shah M, Hochman L, Ankoma-Sey V, DuPont AW, Wong MC, Alexander A, Ke S, DuPont HL. 2017. Randomised clinical trial: faecal microbiota transplantation for recurrent *Clostridium difficile* infection—fresh, or frozen, or lyophilised microbiota from a small pool of healthy donors delivered by colonoscopy. *Aliment Pharmacol Ther* 45:899–908. <https://doi.org/10.1111/apt.13969>.
34. Rajasingham R, Enns EA, Khoruts A, Vaughn BP. 2019. Cost-effectiveness of treatment regimens for *Clostridioides difficile* infection: an evaluation of the 2018 Infectious Diseases Society of America Guidelines. *Clin Infect Dis* 372:825–829.
35. Tan X, Johnson S. 2019. Fecal microbiota transplantation (FMT) for *C. difficile* infection, just say ‘No.’ *Anaerobe* 60:102092. <https://doi.org/10.1016/j.anaerobe.2019.102092>.
36. Tvede M, Rask-Madsen J. 1989. Bacteriotherapy for chronic relapsing *Clostridium difficile* diarrhoea in six patients. *Lancet* i:1156–1160. [https://doi.org/10.1016/S0140-6736\(89\)92749-9](https://doi.org/10.1016/S0140-6736(89)92749-9).
37. Petrof EO, Gloor GB, Vanner SJ, Weese SJ, Carter D, Daigneault MC, Brown EM, Schroeter K, Allen-Vercoe E. 2013. Stool substitute transplant therapy for the eradication of *Clostridium difficile* infection: “RePOOPulating” the gut. *Microbiome* 1:3. <https://doi.org/10.1186/2049-2618-1-3>.
38. Garland JL, Lehman RM. 1999. Dilution/extinction of community phenotypic characters to estimate relative structural diversity in mixed communities. *FEMS Microbiol Ecol* 30:333–343. <https://doi.org/10.1111/j.1574-6941.1999.tb00661.x>.
39. Franklin RB, Garland JL, Bolster CH, Mills AL. 2001. Impact of dilution on microbial community structure and functional potential: comparison of numerical simulations and batch culture experiments. *Appl Environ Microbiol* 67:702–712. <https://doi.org/10.1128/AEM.67.2.702-712.2001>.
40. Auchtung JM, Robinson CD, Britton RA. 2015. Cultivation of stable, reproducible microbial communities from different fecal donors using minibioreactor arrays (MBRAs). *Microbiome* 3:42. <https://doi.org/10.1186/s40168-015-0106-5>.
41. Holmes I, Harris K, Quince C. 2012. Dirichlet multinomial mixtures: generative models for microbial metagenomics. *PLoS One* 7:e30126. <https://doi.org/10.1371/journal.pone.0030126>.
42. Collins J, Auchtung JM, Schaefer L, Eaton KA, Britton RA. 2015. Humanized microbiota mice as a model of recurrent *Clostridium difficile* disease. *Microbiome* 3:35. <https://doi.org/10.1186/s40168-015-0097-2>.
43. Seekatz AM, Aas J, Gessert CE, Rubin TA, Saman DM, Bakken JS, Young VB. 2014. Recovery of the gut microbiome following fecal microbiota transplantation. *mBio* 5:e00893-14. <https://doi.org/10.1128/mBio.00893-14>.
44. Seekatz AM, Theriot CM, Rao K, Chang Y-M, Freeman AE, Kao JY, Young VB. 2018. Restoration of short chain fatty acid and bile acid metabolism following fecal microbiota transplantation in patients with recurrent *Clostridium difficile* infection. *Anaerobe* 53:64–73. <https://doi.org/10.1016/j.anaerobe.2018.04.001>.
45. Antharam VC, Li EC, Ishmael A, Sharma A, Mai V, Rand KH, Wang GP. 2013. Intestinal dysbiosis and depletion of butyrogenic bacteria in *Clostridium difficile* infection and nosocomial diarrhea. *J Clin Microbiol* 51:2884–2892. <https://doi.org/10.1128/JCM.00845-13>.
46. Staley C, Kaiser T, Vaughn BP, Graiziger C, Hamilton MJ, Kabage AJ, Khoruts A, Sadowsky MJ. 2019. Durable long-term bacterial engraftment following encapsulated fecal microbiota transplantation to treat *Clostridium difficile* infection. *mBio* 10:e01586-19. <https://doi.org/10.1128/mBio.01586-19>.
47. Song Y, Garg S, Girotra M, Maddox C, Rosenvinge von EC, Dutta A, Dutta S, Fricke WF. 2013. Microbiota dynamics in patients treated with fecal microbiota transplantation for recurrent *Clostridium difficile* infection. *PLoS One* 8:e81330. <https://doi.org/10.1371/journal.pone.0081330>.
48. Feng Z, Long W, Hao B, Ding D, Ma X, Zhao L, Pang X. 2017. A human stool-derived *Bifidobacterium wadsworthia* strain caused systemic inflammation in specific-pathogen-free mice. *Gut Pathog* 9:59. <https://doi.org/10.1186/s13099-017-0208-7>.
49. Smits WK, Lyras D, Lacy DB, Wilcox MH, Kuijper EJ. 2016. *Clostridium difficile* infection. *Nat Rev Dis Primers* 2:16020. <https://doi.org/10.1038/nrdp.2016.20>.
50. Sun X, Hirota SA. 2015. The roles of host and pathogen factors and the innate immune response in the pathogenesis of *Clostridium difficile* infection. *Mol Immunol* 63:193–202. <https://doi.org/10.1016/j.molimm.2014.09.005>.
51. Schubert AM, Sinani H, Schloss PD. 2015. Antibiotic-induced alterations of the murine gut microbiota and subsequent effects on colonization resistance against *Clostridium difficile*. *mBio* 6:e00974-15. <https://doi.org/10.1128/mBio.00974-15>.
52. Schubert AM, Rogers MAM, Ring C, Mogle J, Petrosino JP, Young VB, Aronoff DM, Schloss PD. 2014. Microbiome data distinguish patients with *Clostridium difficile* infection and non-*C. difficile*-associated diarrhea from healthy controls. *mBio* 5:e01021-14. <https://doi.org/10.1128/mBio.01021-14>.
53. Passmore IJ, Letertre MPM, Preston MD, Bianconi I, Harrison MA, Nasher F, Kaur H, Hong HA, Baines SD, Cutting SM, Swann JR, Wren BW, Dawson LF. 2018. Para-cresol production by *Clostridium difficile* affects microbial diversity and membrane integrity of Gram-negative bacteria. *PLoS Pathog* 14:e1007191. <https://doi.org/10.1371/journal.ppat.1007191>.
54. Winter SE, Winter MG, Xavier MN, Thiennimitr P, Poon V, Keestra AM, Laughlin RC, Gomez G, Wu J, Lawhon SD, Popova IE, Parikh SJ, Adams LG, Tsolis RM, Stewart VJ, Bauml AJ. 2013. Host-derived nitrate boosts growth of *E. coli* in the inflamed gut. *Science* 339:708–711. <https://doi.org/10.1126/science.1232467>.
55. Suez J, Zmora N, Zilberman-Schapira G, Mor U, Dori-Bachash M, Bashardes S, Zur M, Regev-Lehavi D, Briki R-Z, Federici S, Horn M, Cohen Y, Moor AE, Zeevi D, Korem T, Kotler E, Harmelin A, Itzkovitz S, Maharsak N, Shibolet O, Pevsner-Fischer M, Shapiro H, Sharon I, Halpern Z, Segal E, Elinav E. 2018. Post-antibiotic gut mucosal microbiome reconstitution is impaired by probiotics and improved by autologous FMT. *Cell* 174:1406–1423.e16. <https://doi.org/10.1016/j.cell.2018.08.047>.
56. Nagao-Kitamoto H, Leslie JL, Kitamoto S, Jin C, Thomsson KA, Gilliland MG, Kuffa P, Goto Y, Jenq RR, Ishii C, Hirayama A, Seekatz AM, Martens EC, Eaton KA, Kao JY, Fukuda S, Higgins PDR, Karlsson NG, Young VB, Kamada N. 2020. Interleukin-22-mediated host glycosylation prevents *Clostridioides difficile* infection by modulating the metabolic activity of the gut microbiota. *Nat Med* 26:608–617. <https://doi.org/10.1038/s41591-020-0764-0>.
57. Lee YJ, Arguello ES, Jenq RR, Littmann E, Kim GJ, Miller LC, Ling L, Figueroa C, Robilotti E, Perales M-A, Barker JN, Giral S, van den Brink MRM, Pamer EG, Taur Y. 2017. Protective factors in the intestinal microbiome against *Clostridium difficile* infection in recipients of allogeneic hematopoietic stem cell transplantation. *J Infect Dis* 215:1117–1123. <https://doi.org/10.1093/infdis/jix011>.
58. Smillie CS, Sauk J, Gevers D, Friedman J, Sung J, Youngster I, Hohmann EL, Staley C, Khoruts A, Sadowsky MJ, Allegretti JR, Smith MB, Xavier RJ, Alm EJ. 2018. Strain tracking reveals the determinants of bacterial engraftment in the human gut following fecal microbiota transplanta-



- tion. *Cell Host Microbe* 23:229–240.e5. <https://doi.org/10.1016/j.chom.2018.01.003>.
59. Jenior ML, Leslie JL, Young VB, Schloss PD. 2017. *Clostridium difficile* colonizes alternative nutrient niches during infection across distinct murine gut microbiomes. *mSystems* 2:e00063-17. <https://doi.org/10.1128/mSystems.00063-17>.
  60. Lee STM, Kahn SA, Delmont TO, Shaiber A, Esen ÖC, Hubert NA, Morrison HG, Antonopoulos DA, Rubin DT, Eren AM. 2017. Tracking microbial colonization in fecal microbiota transplantation experiments via genome-resolved metagenomics. *Microbiome* 5:50. <https://doi.org/10.1186/s40168-017-0270-x>.
  61. Robinson CD, Auchtung JM, Collins J, Britton RA. 2014. Epidemic *Clostridium difficile* strains demonstrate increased competitive fitness compared to nonepidemic isolates. *Infect Immun* 82:2815–2825. <https://doi.org/10.1128/IAI.01524-14>.
  62. Auchtung TA, Fofanova TY, Stewart CJ, Nash AK, Wong MC, Gesell JR, Auchtung JM, Ajami NJ, Petrosino JF. 2018. Investigating colonization of the healthy adult gastrointestinal tract by fungi. *mSphere* 3:e00092-18. <https://doi.org/10.1128/mSphere.00092-18>.
  63. Auchtung JM, Robinson CD, Farrell K, Britton RA. 2016. MiniBioReactor arrays (MBRAs) as a tool for studying *C. difficile* physiology in the presence of a complex community. *Methods Mol Biol* 1476:235–258. [https://doi.org/10.1007/978-1-4939-6361-4\\_18](https://doi.org/10.1007/978-1-4939-6361-4_18).
  64. Kellermayer R, Nagy-Szakal D, Harris RA, Luna RA, Pitashny M, Schady D, Mir SAV, Lopez ME, Gilger MA, Belmont J, Hollister EB, Versalovic J. 2015. Serial fecal microbiota transplantation alters mucosal gene expression in pediatric ulcerative colitis. *Am J Gastroenterol* 110:604–606. <https://doi.org/10.1038/ajg.2015.19>.
  65. Caporaso JG, Lauber CL, Walters WA, Berg-Lyons D, Huntley J, Fierer N, Owens SM, Betley J, Fraser L, Bauer M, Gormley N, Gilbert JA, Smith G, Knight R. 2012. Ultra-high-throughput microbial community analysis on the Illumina HiSeq and MiSeq platforms. *ISME J* 6:1621–1624. <https://doi.org/10.1038/ismej.2012.8>.
  66. Kozich JJ, Westcott SL, Baxter NT, Highlander SK, Schloss PD. 2013. Development of a dual-index sequencing strategy and curation pipeline for analyzing amplicon sequence data on the MiSeq Illumina sequencing platform. *Appl Environ Microbiol* 79:5112–5120. <https://doi.org/10.1128/AEM.01043-13>.
  67. McMurdie PJ, Holmes S. 2013. phyloseq: an R package for reproducible interactive analysis and graphics of microbiome census data. *PLoS One* 8:e61217. <https://doi.org/10.1371/journal.pone.0061217>.